NeuroImage: Clinical 14 (2017) 591–601

Contents lists available at ScienceDirect

NeuroImage: Clinical

journal homepage: www.elsevier.com/locate/ynicl

Functional connectivity disruptions correlate with cognitive phenotypes in Parkinson's disease

M. Hassan[a,b,*], L. Chaton[e], P. Benquet[a,b], A. Delval[c,d,e], C. Leroy[c,d,e], L. Plomhause[c,d,e], A.J.H. Moonen[g], A.A. Duits[g], A.F.G. Leentjens[g], V. van Kranen-Mastenbroek[g], L. Defebvre[c,d,f], P. Derambure[c,d,e], F. Wendling[a,b], K. Dujardin[c,d,f]

[a] INSERM, U1099, F-35000 Rennes, France
[b] University of Rennes 1, LTSI, F-35000 Rennes, France
[c] University of Lille, U1171 - Degenerative & Vascular Cognitive Disorders, F-59000 Lille, France
[d] INSERM, U1171, F-59000 Lille, France
[e] CHU Lille, Clinical Neurophysiology Department, F-59000 Lille, France
[f] CHU Lille, Neurology and Movement Disorders Department, F-59000 Lille, France
[g] Maastricht University Medical Center, Maastricht, The Netherlands

ARTICLE INFO

Article history:
Received 13 October 2016
Received in revised form 28 February 2017
Accepted 4 March 2017
Available online 6 March 2017

Keywords:
Parkinson's disease
Cognitive deficits
Dense electroencephalography
Brain connectivity
Network measures

ABSTRACT

Cognitive deficits in Parkinson's disease are thought to be related to altered functional brain connectivity. To date, cognitive-related changes in Parkinson's disease have never been explored with dense-EEG with the aim of establishing a relationship between the degree of cognitive impairment, on the one hand, and alterations in the functional connectivity of brain networks, on the other hand.

This study was aimed at identifying altered brain networks associated with cognitive phenotypes in Parkinson's disease using dense-EEG data recorded during rest with eyes closed. Three groups of Parkinson's disease patients ($N = 124$) with different cognitive phenotypes coming from a data-driven cluster analysis, were studied: G1) cognitively intact patients (63), G2) patients with mild cognitive deficits (46) and G3) patients with severe cognitive deficits (15). Functional brain networks were identified using a dense-EEG source connectivity method. Pairwise functional connectivity was computed for 68 brain regions in different EEG frequency bands. Network statistics were assessed at both global (network topology) and local (inter-regional connections) level.

Results revealed progressive disruptions in functional connectivity between the three patient groups, typically in the alpha band. Differences between G1 and G2 ($p < 0.001$, corrected using permutation test) were mainly frontotemporal alterations. A statistically significant correlation ($\rho = 0.49$, $p < 0.001$) was also obtained between a proposed network-based index and the patients' cognitive score. Global properties of network topology in patients were relatively intact.

These findings indicate that functional connectivity decreases with the worsening of cognitive performance and loss of frontotemporal connectivity may be a promising neuromarker of cognitive impairment in Parkinson's disease.

1. Introduction

Pathological perturbations of the brain are rarely limited to a single region. Local dysfunctions often propagate via axonal paths and affect other regions, resulting in large-scale network alterations (Fornito et al., 2015). Over recent years, the identification of alterations in functional and structural networks from neuroimaging data became one of the most promising prospects in brain diseases research. Indeed, neuroimaging helps investigation of the pathophysiological mechanisms in vivo, and results from previous studies have shown that brain network topology tends to shape neural responses to damage (Fornito and Bullmore, 2015; Fornito et al., 2015). In graph-theory approaches, brain networks are characterized as sets of nodes (brain regions) connected by edges (Bullmore and Sporns, 2009). Once nodes and edges have been defined from the neuroimaging data, network topological properties (organization) can be studied by graph-theory metrics and functional connectivity by network-based statistics. Using different neuroimaging techniques (functional magnetic resonance imaging -fMRI-, magneto/electro-encephalography -M/EEG-), these combined approaches have been used to characterize functional changes associated with conditions such as Alzheimer's disease (He et al., 2008; Lo et al., 2010; Mallio et al., 2015; Stam et al., 2007), Parkinson's disease (Baggio et al., 2015), Huntington's disease (Harrington et al., 2015), epilepsy

* Corresponding author at: INSERM, U1099, F-35000 Rennes, France.
E-mail address: mahmoud.hassan@univ-rennes1.fr (M. Hassan).

http://dx.doi.org/10.1016/j.nicl.2017.03.002

(Liao et al., 2010; Ponten et al., 2007; Zhang et al., 2011), schizophrenia (Fornito et al., 2011) and autism (Guye et al., 2010; Li et al., 2014).

Parkinson's disease is the second most common neurodegenerative disease after Alzheimer's disease and affects >1% of the population over the age of 60 (de Lau and Breteler, 2006). Besides the hallmark motor symptoms (rest tremor, hypokinesia, rigidity and postural instability), cognitive deficits are common in Parkinson's disease. They are however heterogeneous in their clinical presentation and progression (Halliday and McCann, 2010; Reid et al., 2011; Tröster, 2011). The early detection and the quantitative assessment of these cognitive deficits is a crucial clinical issue, not only for characterizing the disease but also its progression. Several studies have previously reported alterations in brain network organization and functional connectivity associated with cognitive deficits in Parkinson's disease using fMRI, MEG and standard EEG (Baggio et al., 2014; Baggio et al., 2015; Bertrand et al., 2016; Bosboom et al., 2009; Lopes et al., 2017; Olde Dubbelink et al., 2014; Skidmore et al., 2011). So far, cognitive-related changes in brain connectivity in Parkinson's disease have never been explored with dense-EEG with the aim of establishing a relationship between i) the degree of cognitive impairment, on the one hand, and ii) spatially-localized alterations in the functional connectivity of brain networks, on the other hand.

In this study, we recorded dense-EEG during eye-closed, resting state in Parkinson's disease patients whose cognitive profile has been identified by a cluster analysis on the results of an extensive battery of neuropsychological tests (Dujardin et al., 2015). Our main objective was to detect alterations in functional networks according to the severity of cognitive impairment; essentially those related to mild cognitive deficits, which represent a serious challenge nowadays. To do so, functional connectivity was investigated using a 'EEG source connectivity' method (Hassan et al., 2015a; Hassan et al., 2014). As compared with fMRI studies of functional connectivity, a unique advantage of this method is that networks could be directly identified at the cerebral cortex level from scalp EEG recordings, which consist in direct measurement of neuronal activity, in contrast with blood-oxygen-level-dependent (BOLD) signals. Our main hypothesis was that EEG connectivity was progressively altered as cognitive impairment worsened. More specifically, we assumed that brain-network organization parameters would differ according to the cognitive status of the patients and that functional connectivity would be more altered in patients with cognitive deficits compared to cognitively intact patients.

2. Methods

2.1. Participants

The data used in this analysis were acquired (from March 2013 to August 2014) in a cross-sectional study of two independent European movement disorder centers: in Lille, France and in Maastricht, the Netherlands (Dujardin et al., 2015). One hundred fifty-six patients with idiopathic Parkinson's disease defined according to the UK Brain Bank criteria for idiopathic Parkinson's disease (Gibb and Lees, 1988) were included. None was suffering from a neurological disorder other than Parkinson's disease. Patients with moderate and severe dementia (defined as a score > 1 at the Clinical Dementia Rating (Morris, 1993) and according to the Movement Disorders criteria (Emre et al., 2007)) and those older than 80 years were excluded. Patients with recent (<2-month) changes in their medical treatment were also excluded. All participants gave their informed consent to participation in the study, which had been approved by the local institutional review boards (CPP Nord-Ouest IV, 2012-A 01317-36, ClinicalTrials.gov Identifier: NCT01792843).

Detailed demographic and disease-related variables were recorded. All the patients' medications were checked and doses of antiparkinsonian medication were converted to levodopa equivalent daily dose according to the algorithm by Tomlinson et al. (2010). Severity of motor symptoms was assessed by the score at the Movement Disorders Society - Unified Parkinson Disease Rating Scale (MDS-UPDRS) - part III (Goetz et al., 2008) and disease stage by the Hoehn & Yahr score (Hoehn and Yahr, 2001). The severity of depression, apathy and anxiety symptoms was quantified with the 17-item Hamilton Depression Rating Scale (Hamilton, 1960), the Lille Apathy Rating Scale (Sockeel et al., 2006) and the Parkinson Anxiety Rating Scale (Leentjens et al., 2014), respectively. The presence and severity of hallucinations were checked by the score on the item 1.2 of the MDS-UPDRS.

All participants underwent a comprehensive neuropsychological assessment including tests for global cognition and standardized tests representing five cognitive domains: 1) attention and working memory (Digit span forward and backward (Wechsler, 1981), Symbol Digit Modalities Test (Smith, 1982), 2) executive functions (Trail Making Test B/A ratio (Reitan and Wolfson, 1995), the interference index and the number of errors in the interference condition of a 50-item version of the Stroop word color test and a 1-minute phonemic word generation task performed in single and alternating conditions), 3) verbal episodic memory (Hopkins verbal learning test (Brandt and Benedict, 2001)), 4) language (the 15-item short form of the Boston naming test (Graves et al., 2004) and animal names generation task in 1 min) and 5) visuospatial functions (the short version of the judgment of line orientation test (Benton et al., 1978)). A cluster analysis (based on the k-means method) performed on the neuropsychological variables identified five phenotypes that were used for separating the participants according to their cognitive status: 1) cognitively intact patients with high level of performance in all cognitive domains, 2) cognitively intact patients with only slight mental slowing, 3) patients with mild to moderate deficits in executive functions, 4) patients with severe deficits in all cognitive domains, particularly executive functions, 5) patients with severe deficits in all cognitive domains, particularly working memory and recall in verbal episodic memory (for details, see (Dujardin et al., 2015)).

One hundred thirty-three of these patients had a high-density EEG recording after receiving their usual anti-Parkinson medication and being in their best "on" state. For the purpose of this exploratory EEG study, we decided to merge the two groups of cognitively intact patients and the two groups of patients with severe cognitive deficits in order to consider only overall cognitive profiles. For further analyses, patients will then be separated into three groups: 1) cognitively intact patients (G1), 2) patients with mild to moderate deficits in executive functions (G2), 3) patients with severe cognitive impairment (G3). All participants were assessed after having received their usual anti-parkinsonian medication and were in their "best on" state during the whole duration of EEG recording and neuropsychological assessment.

2.2. Data acquisition and preprocessing

Dense-EEG were recorded with a cap (Waveguard®, ANT software BV, Enschede, the Netherlands) with 128 channels including 122 scalp electrodes distributed according to the international system 10-05 (Oostenveld and Praamstra, 2001), two electro-cardiogram and four bilateral electro-oculogram electrodes (EOG) for vertical and horizontal movements. Electrodes impedance was kept below 10 kΩ. The data were collected in an eye-closed resting-state condition for 10 min with the software BrainVision Recorder (BrainProducts®). Subjects were instructed to do nothing and relax. All recordings were performed between 11:00 and 12:00 a.m. to limit drowsiness. An investigator controlled online the subject and EEG and verbally alerted the subject every time there were signs of drowsiness on the EEG traces or in behavior. Signals were sampled at 512 Hz and band-pass filtered between 1 and 45 Hz. Channels and epochs containing artifacts were automatically and/or manually discarded. The automatic procedures included EOG artifact detection and correction using the method developed in (Gratton et al., 1983), and EEG artifact analysis using a data inspection tracking system to remove data with an amplitude over 90 μV. The automatic

selection was confirmed manually and epochs with remained artifacts (such as movement artifact) were removed. For each participant, we selected the maximum number of four-second segments artifacts-free to perform analyses. An atlas-based approach was used to project EEG sensor signals onto an anatomical framework consisting of 68 cortical regions identified by means of the Desikan-Killiany (Desikan et al., 2006) atlas using Freesurfer (Fischl, 2012), http://freesurfer.net/. (See Table S1 in Supplementary materials for more details about the name of these regions). For this purpose, a template MRI and EEG data were co-registered through identification of the same anatomical landmarks (left and right pre-auricular points and nasion). A realistic head model was built by segmenting the MRI using Freesurfer. The lead field matrix was then computed for a cortical mesh with 15,000 vertices using Brainstorm (Tadel et al., 2011) and OpenMEEG (Gramfort et al., 2010).

2.3. Power spectrum analysis

We used a standard Fast Fourier Transform (FFT) approach for power spectrum analysis with Welch technique and Hanning windowing function (2 s epoch and overlap of 50%). Relative power spectrum was computed for each frequency band [delta (0.5–4 Hz); theta (4–8 Hz); alpha 1 (8–10 Hz); alpha 2 (10–13 Hz); beta (13–30 Hz); gamma (30–45 Hz)], with 0.5 Hz frequency resolution.

2.4. Functional connectivity analysis

Functional connectivity matrices were computed using the 'EEG source connectivity' method (Hassan et al., 2014; Hassan et al., 2015b). It includes two main steps: i) solving the EEG inverse problem

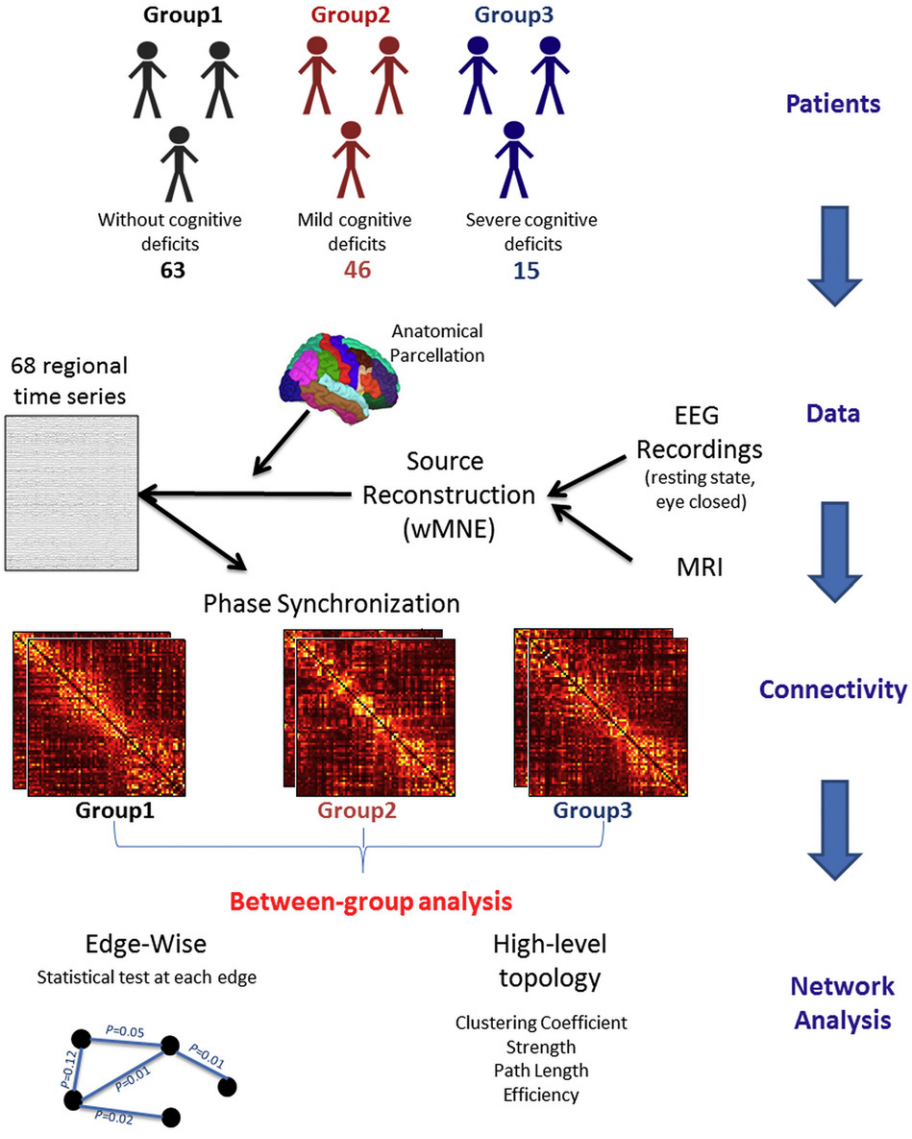

Fig. 1. Structure of the investigation. **Patients** were categorized by their cognitive performance 1) cognitively intact subjects, 2) patients with mild cognitive impairment and 3) patients with severe cognitive impairment. The demographic and clinical features of the three groups are summarized in Table 1. The performance and the neuropsychological test of the three groups are also described in Table 2 (see (Dujardin et al., 2015) for more description about the database). **Data:** Dense-EEGs were recorded using 128 electrodes during resting state (eye closed). The MRIs of the subjects were also available. The cortical sources were reconstructed by solving the inverse problem using the weighted Minimum Norm Estimate (wMNE) method. An anatomical parcellation was applied on the MRI template producing 68 regions of interest (Desikan-Killany atlas) computed using Freesurfer (Fischl, 2012) and then imported for further processing into brainstorm (Tadel et al., 2011). The functional **connectivity** was computed between the 68 regional time series using the Phase Locking Value (PLV) method at six frequency bands: [delta (0.5–4 Hz); theta (4–8 Hz); alpha 1 (8–10 Hz); alpha 2 (10–13 Hz); beta (13–30 Hz); gamma (30–45 Hz)]. The connectivity matrices were compared between the groups using two level of **network analysis** i) High-level topology where we computed four network metrics: the clustering coefficient, the strength, the characteristic path length and the global efficiency and ii) edge-wise analysis where we computed the between-group statistical analysis at the level of each connections in the network using the Network Based Statistics (NBS) approach (Zalesky et al., 2010a).

to reconstruct the temporal dynamics of the cortical regions and ii) measuring the functional connectivity between these reconstructed regional time series (Fig. 1). The weighted Minimum Norm Estimate (wMNE) was used to reconstruct the dynamics of the cortical sources. The functional connectivity was then computed between the reconstructed sources using the phase synchronization (PS) method. To measure the PS, the phase locking value (PLV) method was used as described in (Lachaux et al., 1999). This measure (range between 0 and 1) reflects true interactions between two oscillatory signals through quantification of the phase relationships. The PLVs were estimated at six frequency bands [delta (0.5–4 Hz); theta (4–8 Hz); alpha1 (8–10 Hz); alpha2 (10–13 Hz); beta (13–30 Hz); gamma (30–45 Hz)]. The choice of wMNE/PLV was supported by two comparative analyses performed in (Hassan et al., 2014; Hassan et al., 2016) that reported the superiority of wMNE/PLV over other combinations of five inverse algorithms and five connectivity measures. Briefly, in (Hassan et al., 2016), the network identified by each of the inverse/connectivity combination used to identify cortical brain networks from scalp EEG was compared to a reference network. The combination that showed the highest similarity between scalp-EEG-based network and reference network (using a network similarity algorithm) was considered as the optimal combination. This was the case for the wMNE/PLV.

The inverse solutions were computed using Brainstorm (Tadel et al., 2011). The network measures and network visualization were performed using BCT (Rubinov and Sporns, 2010) and EEGNET (Hassan et al., 2015b) respectively. See Fig. S1 in the Supplementary materials for more details about the dense-EEG source connectivity method.

2.5. Network analysis

Networks can be illustrated by graphs, which are sets of nodes (brain regions) and of edges (connectivity values) between those nodes. We constructed graphs of 68 nodes (i.e. the 68 previously identified cortical regions) and used all information from the functional connectivity (phase locking value) matrix. This gave fully connected, weighted and undirected networks, in which the connection strength between each pair of vertices (i.e. the weight) was defined as their connectivity value. Several metrics can be calculated to characterize weighted networks (for a wide-ranging overview, see (Rubinov and Sporns, 2010)). Here, we examined networks analysis at two levels:

i) *Global level* reflected the overall network organization where we computed several measures including path length (P_L), clustering coefficient (C_c), strength (Str) and global efficiency (E_G) (more details are provided in Supplementary materials). All above mentioned network measures depend on the edge weights. By consequence, they were normalized. They were expressed as a function of measures computed from random networks. We generated 500 surrogate random networks derived from the original ones by randomly reshuffling the edge weights. The normalized values were computed by dividing the original value by the average of the values computed on the randomized graphs as reported in (Olde Dubbelink et al., 2014).
ii) *Edge-wise level* reflected functional connectivity through the measure of each of the correlation values (weights) between the different brain regions.

2.6. Statistical analyses

Edge-wise connectivity was characterized using the network-based statistic (Zalesky et al., 2010a). To compute the network-based statistic, an ANCOVA analysis was fitted to each of the $(N^2 - N)/2 = 2278$ edges (phase synchronization values) in the (68×68) functional connectivity matrix, yielding a p value matrix indicating the probability of rejecting the null hypothesis at each edge. A component-forming threshold, T, was applied to each p value, and the size of each connected element in these thresholded matrices was obtained. The size of the components was then compared with a null distribution of maximal component sizes obtained using permutation testing to obtain p values corrected for multiple comparisons (Zalesky et al., 2010a). The NBS method finds subnetworks of connections significantly larger than would be expected by chance (see (Zalesky et al. (2010a) for more details). In line with (Fornito et al., 2011), here we report results for a threshold that retain only edges with $p < 0.005$. Results at higher ($p < 0.01$) and lower ($p < 0.001$) threshold values are reported in Figs. S3 and S4 respectively in Supplementary materials to show sensitivity to parameter sets.

Age and duration of formal education were entered as confounding factors in the ANCOVA for both spectral and connectivity analyses. The statistical analyses were performed using the SPSS Statistics 20.0 software package (IBM Corporation). A significance level of 0.01 (two-tailed) was applied. Corrections for multiple testing were applied using Bonferroni approach.

3. Results

3.1. Demographic and clinical characteristics

After discarding nine EEG recordings due to a lot of artifacts, 124 patients participated in the study and were categorized in 3 different groups (G1, G2, G3), based on their performance at the comprehensive neuropsychological test battery. Their demographical and clinical characteristics are shown in Table 1 and results of neuropsychological assessment are shown in Table 2. Significant between-group differences were observed for age, duration of formal education, severity of apathy symptoms and frequency of hallucinations.

3.2. Power-based and network-based topology analyses

The results of the frequency-based analysis are summarized in Fig. 2. In the alpha 1, alpha 2, beta, and gamma frequency bands, there was a progressive decrease in the power spectral density as cognitive impairment worsened (from G1 to G3). At the opposite, in the delta and theta frequency bands, there was an increase in the power spectral as cognitive impairment worsened (from G1 to G3). Significant differences were

Table 1
Demographic and clinical features of the three patient subgroups. **MDS_UPDRS3** = Movement Disorders Society sponsored revision of the Unified Parkinson's Disease Rating Scale-Part III (severity of motor symptoms); **LEDD** = Levodopa Equivalent Daily Dose; **MMSE** = Mini Mental State Examination; **MDRS** = Mattis dementia rating scale.

N = 124	G1	G2	G3	*p*
	Mean (*SD*)	Mean (*SD*)	Mean (*SD*)	value
n (%)	63 (50.81)	46 (37.10)	15 (12.10)	
Demographic				
Sex (% male)	73.02	63.04	80	0.358
Handedness (% right)	84.12	91.3	93.33	0.362
Age (y)	63.53 (*7.97*)	67.29 (*7.73*)	70.07 (*6.01*)	0.003
Formal education (y)	13.32 (*3.68*)	11.52 (*3.56*)	9.47 (*2.23*)	<0.001
Clinical				
Disease duration(y)	8.05 (*6.43*)	8.8 (*4.97*)	10.6 (*6.23*)	0.317
MDS_UPDRS3 score	27.86 (*11.91*)	28.87 (*11.08*)	32 (*18.15*)	0.514
Hoehn & Yahr stage	2.02 (*0.5*)	2.24 (*0.63*)	2.13 (*0.74*)	0.168
Medication				
LEDD (mg/day)	712.5 (*548.46*)	913.15 (*599.75*)	820.88 (*275.97*)	0.167
Neuropsychiatry				
Hamilton depression rating scale	5.44 (*4.87*)	6.22 (*4.04*)	5.33 (*4.25*)	0.637
Lille apathy rating scale	−26.71 (*6.3*)	−22.72 (*6.93*)	−19.93 (*8.33*)	<0.001
Hallucinations (%)	4.76	17.39	33.33	
Cognition				
MMSE (/30)	28.6 (*1.44*)	27 (*2.19*)	24.13 (*3.42*)	<0.001
Mattis DRS (/144)	140.37 (*3.12*)	134.5 (*5.41*)	124.2 (*9.17*)	<0.001

Table 2
Performance (mean and standard deviation) at the neuropsychological tests of the three patients subgroups. **WAIS-R** = Wechsler for adults intelligence scale revised; **SDMT** = Symbol digit modalities test; **HVLT** = Hopkins verbal learning test.

N = 156	G1 Mean (*SD*)	G2 Mean (*SD*)	G3 Mean (*SD*)	*p* value	Post-hoc test
Attention and working memory					
WAIS-R forward digit (/14)	8.30 (*1.96*)	6.93 (*2.30*)	6.33 (*2.58*)	0.001	1 >2,3
WAIS-R backward digit (/14)	6.38 (*1.47*)	4.96 (*1.69*)	3.47 (*1.51*)	<0.0001	1 > 2,3; 2 > 3
SDMT: number in 90 s	48.59 (*8.07*)	32.98 (*7.03*)	15.73 (*10.11*)	<0.0001	1 > 2,3; 2 > 3
Executive functions					
Trail Making Test (time B/time A)	2.36(*0.69*)	2.84 (*0.81*)	2.58 (*1.29*)	0.013	1 > 2
Stroop: interference index	1.62 (*0.26*)	2.10 (*0.75*)	2.57 (*1.20*)	<0.0001	1 > 2,3; 2 > 3
Stroop: errors	0.65 (*1.14*)	3.91 (*4.48*)	17.47 (*14.46*)	<0.0001	1 > 2,3; 2 > 3
Phonemic fluency: words in 60 s	15.00 (*4.00*)	10.80 (*3.96*)	7.00 (*3.29*)	<0.0001	1 > 2,3; 2 > 3
Alternating fluency: words in 60 s	13.79 (*3.70*)	8.96 (*3.27*)	5.87 (*3.25*)	<0.0001	1 > 2,3; 2 > 3
Episodic memory					
HVLT learn1 (/12)	7.22 (*1.52*)	5.30 (*2.10*)	3.27 (*1.62*)	<0.0001	1 > 2,3; 2 > 3
HVLT learn total (/36)	27.44 (*3.74*)	22.76 (*4.00*)	15.47 (*3.3*)	<0.0001	1 > 2,3; 2 > 3
HVLT delayed recall (/12)	9.78 (*1.86*)	8.02 (*1.91*)	3.93 (*2.60*)	<0.0001	1 > 2,3; 2 > 3
HVLT recognition hits (/12)	11.46 (*0.86*)	11.09 (*1.15*)	9.53 (*1.92*)	0.0005	1 > 3; 2 > 3
HVLT number of intrusions	1.21 (*0.90*)	2.46 (*3.20*)	3.00 (*2.10*)	0.008	1 > 2,3
Language					
Boston naming test (/15)	13.46 (*1.59*)	11.33 (*2.55*)	10.67 (*2.89*)	<0.0001	1 > 2,3
Semantic fluency (animals in 60 s)	22.94 (*4.77*)	14.74 (*3.89*)	9.73 (*5.45*)	<0.0001	1 > 2,3; 2 > 3
Visuospatial functions					
Judgment of line orientation	12.17 (*2.61*)	10.74 (*3.04*)	7.60 (*3.02*)	<0.0001	1 > 2,3; 2 > 3

observed between G1 and G3 and between G2 and G3 in the delta, theta and beta frequency bands ($p < 0.01$, Bonferroni corrected for each comparison). We did not observe any significant difference between G1 and G2 whatever the frequency band. Regarding the network-based topology analysis, the four metrics (P_L, C_c, Str and E_G) tended to decrease as cognitive impairment worsened (from G1 to G3), at all the frequency bands, without any significant differences (see Fig. S2 in the Supplementary materials).

3.3. Edge-wise analysis

Fig. 3 shows the results of the edge-wise analysis performed using the NBS toolbox. The statistical tests (ANCOVA, corrected by permutation test) were applied to each connection in the networks computed at all the frequency bands (delta, theta, alpha 1, alpha 2, beta and gamma). Significant differences were found only between networks computed at the EEG alpha band (alpha 1 and alpha 2).

Concerning the alpha 2 networks, the difference between G1 and G2 revealed that one connected component comprising 49 edges and 36 regions was statistically significant ($p = 0.03$, corrected using permutation test, Fig. 3A). For all these edges, the connectivity was significantly lower in G2 than G1. To better understand the regional distribution of these connections, we classified each region as belonging to one of five broad scalp areas: frontal, temporal, parietal, occipital or central. We then categorized each edge in the affected subnetwork on the basis of the areas they connected (e.g., fronto-temporal, temporo-parietal, etc.) and counted the proportion of edges falling into each category. When comparing G1 and G2, most reduced connections in G2 were fronto-temporal (36%). Similar results were obtained across different values of threshold (see Figs. S3 and S4 in Supplementary materials).

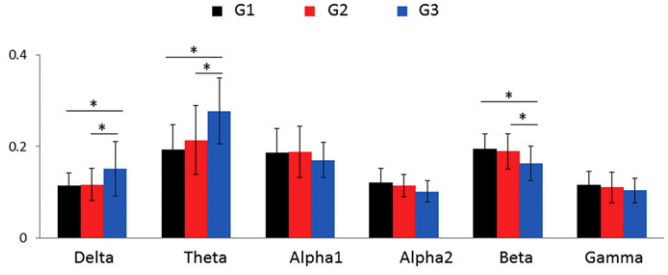

Fig. 2. A. Frequency based analysis: mean ± standard deviation values of the power spectral density for each group of patients at six frequency bands: [delta (0.5–4 Hz); theta (4–8 Hz); alpha1 (8–10 Hz); alpha2 (10–13 Hz); beta (13–30 Hz); gamma (30–45 Hz)]. The * denotes a *p* value < 0.01, Bonferroni corrected.

When comparing G2 and G3, one connected component comprising 125 edges and 57 regions was statistically significant ($p < 0.001$, corrected using permutation test, Fig. 2B). For all edges, the functional connectivity was significantly reduced in G3. Most of these altered connections were fronto-central (20%), temporo-frontal (12%), fronto-frontal (12%) and occipito-central (12%). Similar results were obtained across different values of threshold (see Figs. S3 and S4 in Supplementary materials).

One connected component, comprising 229 edges and 57 regions was significant between G1 and G3 ($p < 0.001$, corrected using permutation test, Fig. 3C). Most of these decreased connections were parieto-frontal (14%), fronto-central (14%) and temporo-frontal (13%). Similar results were obtained across different values of threshold (see Figs. S3 and S4 in Supplementary materials).

Concerning the alpha1 networks, results showed significance difference between G2 and G3 with a component of 60 nodes and 320 edges ($p < 0.001$, Fig. 4A). These alterations mainly concerned temporo-frontal (20%), temporo-temporal (15%) and fronto-central (10%) connections.

In addition, one connected component, comprising 123 edges and 47 regions showed significant differences between G1 and G3 ($p = 0.004$, Fig. 4B). Most of these decreased connections were temporo-frontal (24%), fronto-central (10%) and temporo-temporal (10%). No significant difference was observed between G1 and G2 at the alpha1 frequency band.

3.4. Correlations between brain connectivity and performance at the neuropsychological tests

To assess the relationships between functional connectivity and Parkinson's disease patients cognitive performance, we on the subnetwork showing a significant difference between G1 and G2 (Fig. 3A). We reasoned that these 49 edges were the most relevant for detecting

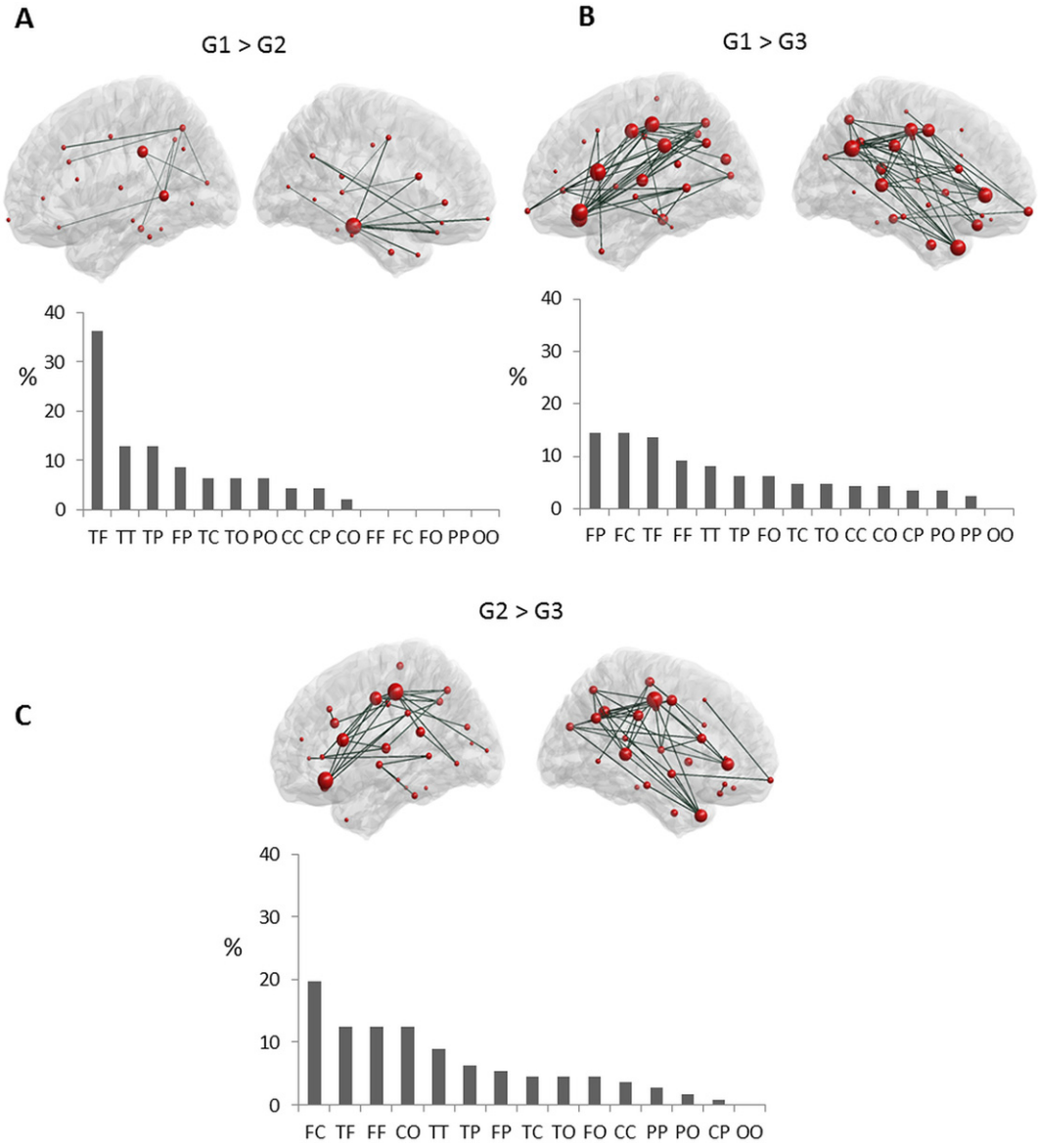

Fig. 3. Edge-wise analysis (alpha 2). Subnetworks of functional connections showing a significant difference between the three groups at alpha 2. At each part, the top row presents graph-based representations of these subnetworks, with each region represented as a red sphere plotted according to the stereotactic coordinates of its centroid, and each suprathreshold edge represented as a dark green line. The size of the node represents the number of significantly different connections from the node itself. For all edges, connectivity was higher in G1 > G2 (A), G1 > G3 (B) and G2 > G3 (C). Bottom row presents the proportion (%) of each type of connection in each subnetwork, as categorized according to the lobes each edge interconnects. F: Frontal, T: Temporal, P: Parietal, C: Central, and O: Occipital.

a marker of cognitive impairment in Parkinson's disease. For each network, we derived an Edge-Wise Connectivity Index (EWCI) as the sum of the weights of the significant subnetwork:

$$EWCI = \left(\sum_{i}^{N} W_i\right) \times 100$$

where W_i represents the weight of the edge i in the significant subnetwork and N is the number of edges in the subnetwork (N = 49 in this case). For the correlation analysis, we used the three most discriminant neuropsychological tests identified by the discriminant factorial analysis (see, Dujardin et al., 2015). It included the number of correct responses at the symbol digit modalities test (SDMT), the number of errors at the Stroop test and animal fluency in 60 s. Z-scores were calculated for each of these tests and the cognitive score used for the correlation analysis (Spearman ρ) was the sum of these Z-scores. Results are shown in Fig. 5. When considering all groups, the EWCI was significantly correlated with the cognitive score ($\rho = 0.49$, $p < 0.01$), Fig. 5A. To ensure that the correlation was not only driven by G3 (as it might be perceived in the figure), we computed the correlation between EWCI and cognitive score for G1 and G2, results show that the association remains significant ($\rho = 0.37$, $p < 0.01$), Fig. 5B.

4. Discussion

Brain disorders are rarely limited to a single region. Local dysfunctions often propagate to affect other regions, resulting in large-scale brain network alterations (Fornito et al., 2015). This is particularly true in neurodegenerative diseases. Therefore, the identification of disruptions in whole-brain functional networks from noninvasive recordings and their relationships with cognitive impairment is a very important and challenging issue. Indeed, discovering functional connectivity abnormalities correlated with unfavorable disease progression could help prognosis of cognitive decline with the identification of markers for disease progression, and guide treatment instauration.

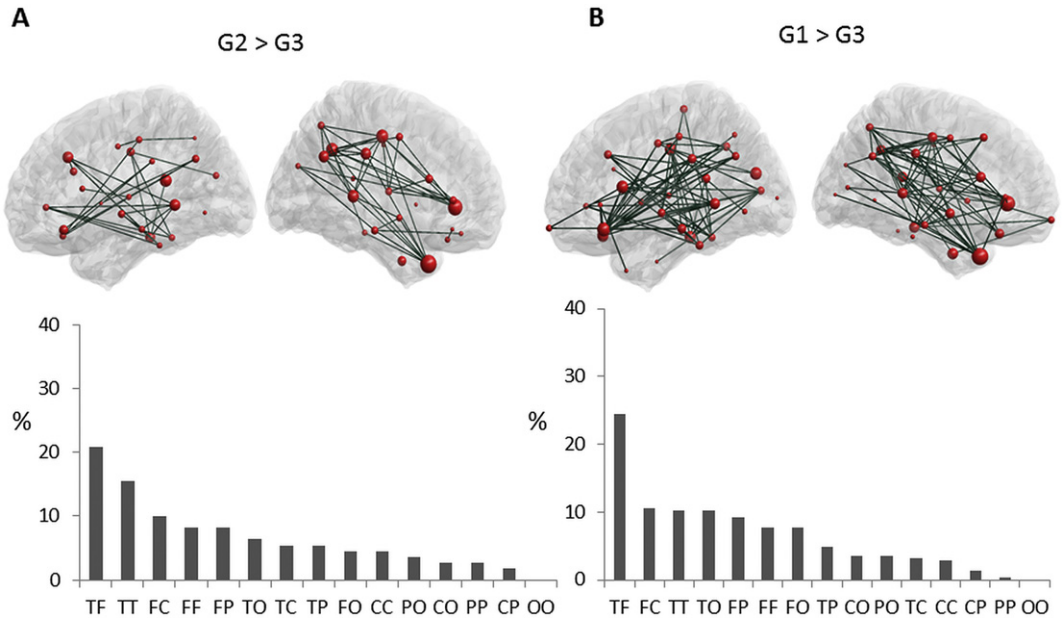

Fig. 4. Edge-wise analysis (alpha 1). Subnetworks of functional connections showing a significant difference between the three groups at alpha 1. At each part, the top row presents graph-based representations of these subnetworks, with each region represented as a red sphere plotted according to the stereotactic coordinates of its centroid, and each suprathreshold edge represented as a dark green line. The size of the node represents the number of significantly different connections from the node itself. For all edges, connectivity was higher in G2 > G3 (A) and G1 > G3 (B). Bottom row presents the proportion (%) of each type of connection in each subnetwork, as categorized according to the lobes each edge interconnects. F: Frontal, T: Temporal, P: Parietal, C: Central, and O: Occipital.

Here, based on scalp dense-EEG recordings, we detected alterations in functional networks associated with cognitive deficits in patients with Parkinson's disease. Using the edge-wise analysis, we highlighted disturbances in functional connectivity in the alpha 2 frequency band even when cognitive deficits were still mild (by comparison of G1 and G2).

Although using EEG to detect cognitive decline in PD is not new in itself, the originality of this work is twofold. On one hand, most previous studies (using EEG) focused on comparing groups such as healthy controls vs. PD with or without dementia. Here, the data came from a large group of Parkinson's disease patients who underwent a comprehensive neuropsychological assessment and were categorized in different cognitive phenotypes (cognitively intact patients, patients with mild to moderate deficits mainly in executive functions and patients with severe cognitive deficits in all cognitive domains including memory) by a data-driven clustering approach (Dujardin et al., 2015). Hence, the differences of functional connectivity between groups are linked to different cognitive profiles that were not defined a priori. On the other hand, most previous studies tried detecting differences in the EEG frequency-bands power and a common finding was the slowing of EEG with PD progression (Kamei et al., 2010). This approach failed to detect differences between the G1 and G2, although such marker of mild cognitive deficits is a real challenge. Here, we focused on the detection of EEG functional connectivity disruptions between different brain regions of networks associated to PD patients with different cognitive phenotypes. Previously, functional connectivity was usually computed at the scalp (electrodes) level. However, the EEG scalp level connectivity does not allow interpretation of anatomically interacting brain areas as they are severely corrupted by the volume conduction effects, see (Brunner et al., 2016; Schoffelen and Gross, 2009; Van de Steen et al., 2016) for recent discussion. Here, EEG source connectivity approach was used to identify functional networks at the cortical level from scalp dense-EEG recordings. This method was first evaluated for its capacity to reveal relevant networks in a picture naming task (Hassan et al., 2014) and was then extended to the tracking of the spatiotemporal dynamics of reconstructed brain networks (Hassan et al., 2015a; Hassan and Wendling, 2015). Graph theory metrics were firstly computed reflecting the global topology characteristics of the network. This approach also failed to detect significant differences between the three groups. Finally, assessment of the functional connectivity between cortical regions (called edge-wise analysis) showed a significant difference between each of the three cognitive phenotypes. These findings

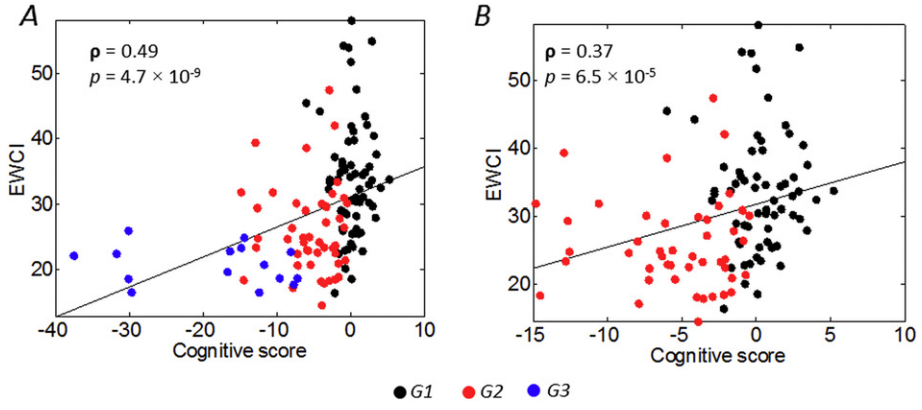

Fig. 5. Scatterplot of the association between the cognitive score and the edge-wise connectivity index for the A) G1, G2 and G3 and B) G1 and G2.

indicate that functional connectivity decreases with the worsening of cognitive performance and loss of connectivity between the frontal and temporal regions may be a marker of mild to moderate cognitive deficits in Parkinson's disease. Results are further discussed hereafter.

4.1. EEG and cognitive impairment

EEG has increasingly been used to describe cognitive impairment in neurodegenerative disorders (Fonseca et al., 2009; Roh et al., 2011). Resting-state recordings from Alzheimer's disease patients were characterized by a shift to lower frequencies (Bennys et al., 2001; Czigler et al., 2008; Penttila et al., 1985). Similar findings were reported in Parkinson's disease when comparing cognitively intact patients, patients with mild cognitive impairment and with dementia (Bousleiman et al., 2014; Caviness et al., 2007). A slowing of EEG was even found in early-untreated Parkinson's disease patients without dementia, but with deficits in executive functions (Kamei et al., 2010; Stoffers et al., 2007). The comparison between Alzheimer's disease and Parkinson's disease patients with dementia with a similar severity of dementia (based on the score at the MMSE) showed higher EEG slowing in Parkinson's disease patients with dementia (Babiloni et al., 2011; Fonseca et al., 2013). A slowing of EEGs (mainly in the theta power) was also observed in Parkinson's disease and Alzheimer's disease at early stage of the disease (Benz et al., 2014). Our results agree with most of the reported studies. We observed a shifting towards lower frequencies from G1 to G3 and G2 to G3 mainly in delta and theta frequency bands. We also observed an increase in the beta band. A possible explanation of these observations is that disruption of alpha 1 (low alpha) and theta rhythms is due to a phenomena of degeneration of the ascending diffuse projection systems of attention (Klimesch, 1999). Beta oscillations may be altered by intrinsic cortical pathology (Dubbelink et al., 2013).

4.2. Functional connectivity deficits in Parkinson's disease

Considering the brain as a very complex network, recent studies have started to focus on modifications in functional connectivity to extend our understanding of neurodegeneration (see review in (Pievani et al., 2011)). Our results showed a tendency to decreasing in the global topological graph features from G1 to G3 but without any significant differences between the groups. Previous studies have reported loss in network efficiency and hubs in the EEG alpha frequency bands in patients with Lewy bodies dementia in comparison with healthy controls and Alzheimer's disease patients (van Dellen et al., 2015). In a four-year follow-up study of Parkinson's disease patients with MEG recording, reduced node clustering for all frequencies and loss of global network efficiency in alpha frequency band were reported to be related with cognitive decline (Olde Dubbelink et al., 2014).

The absence of significant changes at the level of network global features (averaged over the whole brain) between groups can be explained by the high heterogeneity of the metric values across the brain regions. Nevertheless, a node-wise analysis (statistical test at each node) using these features did not show also significant difference between the groups. It is possible that the normalized features used here (C_G, Str, P_L and E_G) were not sensitive to detect the reorganization in the brain networks of the different groups and therefore other advanced node-level metrics may possibly detect the global (or local) alterations in the networks.

Using the edge-wise analysis, we observed significant differences in alterations in the functional networks at the alpha 1 (8–10 Hz) and alpha 2 (10–13 Hz) frequency bands. Alterations in the alpha band were observed by many previous studies such as those reporting a loss in MEG functional connectivity in demented patients (Bosboom et al., 2009), a reduction in the global coherence (Andersson et al., 2008; Franciotti et al., 2006) and a loss in EEG network efficiency and hubs (van Dellen et al., 2015) in dementia with Lewy bodies and, very recently, a decrease in local integration at the alpha1 frequency bands between cognitively intact and demented Parkinson's disease patients (Utianski et al., 2016). Observing significant alteration between G1 and G2 only in the alpha band was not surprising. The alpha wave is very dominant during eye close resting state reflecting the attentional capacity of the subject (alpha 1) and the integration of the sensory motor and semantic information (alpha 2) via the activation of the thalamo-cortical and cortico-cortical connections (Klimesch, 1999; Steriade et al., 1990). However, the other frequency bands are less dominant during rest (eye closed). For instance, beta and gamma are more associated with cognitive tasks and reflect the local information processing (segregation).

The observed differences between the G1 and G2 were mainly fronto-temporal. A key issue here is that these alterations in connectivity were observed when cognitive deficits are still moderate. Similar fronto-temporal alterations were also previously observed in Alzheimer's disease patients using structural (Zhang et al., 2009) and functional (de Haan et al., 2009) connectivity. MEG studies showed also loss of frontotemporal functional connectivity at the alpha band in Parkinson's disease patients with dementia (Bosboom et al., 2009). These observations are in line with results of structural MRI studies showing early atrophy of temporal and frontal lobes in Parkinson's disease patients with mild cognitive impairment and more widespread atrophy in Parkinson's disease patients with dementia (Beyer et al., 2007; Song et al., 2011). They also agree with neuropathological observations that Lewy bodies pathology first invades the neocortex through these same regions (Braak and Del Tredici, 2009; Braak et al., 2003). We also observed that the alterations in functional connectivity observed in the group of patients with severe deficits (G3) involved more spatially distributed networks, mainly fronto-parietal and fronto-central.

In contrast to our results and those of many other studies, a trend towards an increase in cortico-cortical functional connectivity was reported in Parkinson's disease patients early in the course of the disease compared with healthy controls in the alpha 1, alpha 2, beta and theta frequency bands using MEG (Stoffers et al., 2008). The significance of this increased synchronization between cortical regions remains ambiguous. The absence of a healthy control group in our study does not allow us to verify the existence of such “over-connectivity” at early stages of Parkinson's disease. It is however likely that the observed modifications in the functional network in Parkinson's disease vary depending on the severity of cognitive decline as discussed in (Berendse and Stam, 2007). Only a follow-up of our patients could shed light on these issues.

Although the emerging evidence of considering PD and other neurodegenerative diseases as network diseases drove our analysis, it is worth mentioning here that other fMRI–based approaches also exist for characterizing PD progression without looking at the functional/structural connectivity between brain regions. These signal-amplitude-oriented approaches were applied to resting state BOLD time series by computing of the Amplitude of the Low Frequency Fluctuation (ALFF) of the BOLD signals in order to build a Reliability Mapping of Regional Differences (RMRD) that may help to classify PD from controls (Skidmore et al., 2013). Adapting those approaches to EEG sources and comparing with network-based results could be of interest for further investigation.

4.3. Limitations

Firstly, patients were initially separated into five ‘clusters’ according to their cognitive status, for details, see (Dujardin et al., 2015). As explained in the methods section, patients from clusters 1 and 2 were combined into one group of cognitively intact patients (G1) since we wanted to differentiate the groups according to overall efficiency. However, a further investigation of the differences in functional EEG connectivity between these two clusters could be of interest to test the hypothesis that mental slowing may contribute to be an early marker of cognitive impairment in Parkinson's disease. Moreover, due to the

small number of patients in each cluster after excluding those with unusable recording due to artifacts, patients from clusters 4 and 5 were combined into one group with severe cognitive deficits although their profile were quite different. Again, further investigations are needed to determine whether these profiles are also associated with differences in functional EEG connectivity.

Secondly, although inclusion was prospective, the male/female ratio was higher than usually in our patient group. This may have influenced our results although, up to now, there is no evidence of a sex effect on EEG characteristics of PD patients. Thirdly, our study did not include a group of healthy control subjects. Therefore, the comparison between the networks from patient groups with a reference network was not possible. As our main objective was to discover markers able to detect early cognitive decline in Parkinson's disease patients, we used the group of cognitively intact patients (G1) as a reference and analyses were adjusted on age and education. Moreover, our patient groups did not differ in disease duration and severity of the motor symptoms (assessed by the score at the MDS-UPDRS III scale). Despite between-group differences, apathy and hallucinations were not considered as nuisance factors in our analyses. Indeed, we considered that lack of initiative, reduction of interests and loss of insight may be symptoms of cognitive impairment since both apathy and hallucinations are embedded with cognitive impairment in Parkinson's disease. Adjusting on these variables, in addition to reduce statistical power, would have removed useful information from our analyses.

Fourthly, regarding the methodological issues, a priori anatomic template to define the network nodes was used in our analyses. This approach is commonly used in the literature (Achard et al., 2006; Fornito et al., 2011; Lynall et al., 2010). Nevertheless, further work examining the effects of template selection on reported findings will be important to determine their generalizability (Zalesky et al., 2010b). Another problem when computing the connectivity at the source level is the 'spatial leakage' as the reconstruction of true dipole sources from the scalp signals will be spread over numerous voxels.

In this context, few strategies have been proposed to tackle this issue and they mainly intended to remove the zero-lag correlations before performing any connectivity analysis (Brookes et al., 2012; Colclough et al., 2015; Hipp et al., 2012). Others suggested keeping only the long-range connections (de Pasquale et al., 2012). However, these methods suppress possible significant correlations that might happen at zero-lag (Finger et al., 2016). Here, we used the phase locking value. Our choice was supported by two comparative studies using simulated (Hassan et al., 2016) and real data (Hassan et al., 2014). Both analyses showed that PLV has the highest performance among all the tested methods. Even though the PLV does not correct for spatial leakage, it was recently shown to provide highest performance among many other connectivity measures (even those correcting for spatial leakage such as the imaginary part of the coherence) (Finger et al., 2016). These authors also showed that the zero lag correlations are crucial when analyzing the network structural-functional correlations. More recently, a comparative study between different connectivity measures (using the same inverse solution algorithm) did not show a significant difference between PLV and methods correcting for spatial leakage such as the orthogonalized, band limited, power envelop method, when looking at group-level repeatability, within-subject consistency and between-subject consistency in resting state data (Colclough et al., 2016). Nevertheless, we believe that more methodological efforts are still needed to completely overcome issues such as mixing and spatial leakage. The use of multimodal recordings such as EEG/fMRI could be also of interest as it can benefit from the excellent spatial resolution of the fMRI and the excellent time resolution of the EEG and can help to cross-validate of the results from both techniques.

To sum up, we reported a new analysis using dense-EEG source connectivity in Parkinson's disease patients with different cognitive phenotypes. We showed that cognitive impairment in Parkinson's disease is related to functional connectivity alterations. We speculate that this relatively easy-to-use technique is a promising approach not only to detect and characterize alterations in pathological functional networks but also may open perspectives towards designing a neuromarker of cognitive impairment in Parkinson's disease (and other neurodegenerative diseases) from resting-state EEG recordings that could consolidate results of usual neuropsychological tests.

Acknowledgements

This study was funded by the Michael J. Fox Foundation for Parkinson's research. The sponsor was not involved in the study design or in data interpretation, writing of the report or decision to submit the article for publication. This work has also received a French government support granted to the CominLabs excellence laboratory and managed by the National Research Agency in the "Investing for the Future" program under reference ANR-10-LABX-07-01.

Appendix A. Supplementary data

Supplementary data to this article can be found online at http://dx.doi.org/10.1016/j.nicl.2017.03.002.

References

Achard, S., Salvador, R., Whitcher, B., Suckling, J., Bullmore, E., 2006. A resilient, low-frequency, small-world human brain functional network with highly connected association cortical hubs. J. Neurosci. 26, 63–72.
Andersson, M., Hansson, O., Minthon, L., Rosén, I., Londos, E., 2008. Electroencephalogram variability in dementia with lewy bodies, Alzheimer's disease and controls. Dement. Geriatr. Cogn. Disord. 26, 284–290.
Babiloni, C., De Pandis, M.F., Vecchio, F., Buffo, P., Sorpresi, F., Frisoni, G.B., Rossini, P.M., 2011. Cortical sources of resting state electroencephalographic rhythms in Parkinson's disease related dementia and Alzheimer's disease. Clin. Neurophysiol. 122, 2355–2364.
Baggio, H.C., Sala-Llonch, R., Segura, B., Marti, M.J., Valldeoriola, F., Compta, Y., Tolosa, E., Junqué, C., 2014. Functional brain networks and cognitive deficits in Parkinson's disease. Hum. Brain Mapp. 35, 4620–4634.
Baggio, H.C., Segura, B., Sala-Llonch, R., Marti, M.J., Valldeoriola, F., Compta, Y., Tolosa, E., Junqué, C., 2015. Cognitive impairment and resting-state network connectivity in Parkinson's disease. Hum. Brain Mapp. 36, 199–212.
Bennys, K., Rondouin, G., Vergnes, C., Touchon, J., 2001. Diagnostic value of quantitative EEG in Alzheimer's disease. Neurophysiol. Clin. 31, 153–160.
Benton, A.L., Varney, N.R., Hamsher, K.D., 1978. Visuospatial judgment. A clinical test. Arch. Neurol. 35, 364–367.
Benz, N., Hatz, F., Bousleiman, H., Ehrensperger, M.M., Gschwandtner, U., Hardmeier, M., Ruegg, S., Schindler, C., Zimmermann, R., Monsch, A.U., Fuhr, P., 2014. Slowing of EEG background activity in Parkinson's and Alzheimer's disease with early cognitive dysfunction. Front. Aging Neurosci. 6, 314.
Berendse, H.W., Stam, C.J., 2007. Stage-dependent patterns of disturbed neural synchrony in Parkinson's disease. Parkinsonism Relat. Disord. 13 (Suppl. 3), S440–S445.
Bertrand, J.-A., McIntosh, R., Postuma, R.B., Kovacevic, N., Latreille, V., Panisset, M., Chouinard, S., Gagnon, J.-F., 2016. Brain connectivity alterations are associated with dementia in Parkinson's disease. Brain Connect. 6.
Beyer, M.K., Janvin, C.C., Larsen, J.P., Aarsland, D., 2007. A magnetic resonance imaging study of patients with Parkinson's disease with mild cognitive impairment and dementia using voxel-based morphometry. J. Neurol. Neurosurg. Psychiatry 78, 254–259.
Bosboom, J., Stoffers, D., Wolters, E.C., Stam, C., Berendse, H., 2009. MEG resting state functional connectivity in Parkinson's disease related dementia. J. Neural Transm. 116, 193–202.
Bousleiman, H., Zimmermann, R., Ahmed, S., Hardmeier, M., Hatz, F., Schindler, C., Roth, V., Gschwandtner, U., Fuhr, P., 2014. Power spectra for screening parkinsonian patients for mild cognitive impairment. Ann. Clin. Transl. Neurol. 1, 884–890.
Braak, H., Del Tredici, K., 2009. Neuroanatomy and pathology of sporadic Parkinson's disease. Adv. Anat. Embryol. Cell Biol. 201, 1–119.
Braak, H., Del Tredici, K., Rub, U., de Vos, R.A., Jansen Steur, E.N., Braak, E., 2003. Staging of brain pathology related to sporadic Parkinson's disease. Neurobiol. Aging 24, 197–211.
Brandt, J., Benedict, R., 2001. Hopkins verbal learning test-revised. Professional Manual. Psychological Assessment Resources, Inc., Lutz, FL.
Brookes, M.J., Woolrich, M.W., Barnes, G.R., 2012. Measuring functional connectivity in MEG: a multivariate approach insensitive to linear source leakage. NeuroImage 63, 910–920.
Brunner, C., Billinger, M., Seeber, M., Mullen, T., Makeig, S., 2016. Volume conduction influences scalp-based connectivity estimates. Front. Comput. Neurosci. 10.
Bullmore, E., Sporns, O., 2009. Complex brain networks: graph theoretical analysis of structural and functional systems. Nat. Rev. Neurosci. 10, 186–198.
Caviness, J.N., Hentz, J.G., Evidente, V.G., Driver-Dunckley, E., Samanta, J., Mahant, P., Connor, D.J., Sabbagh, M.N., Shill, H.A., Adler, C.H., 2007. Both early and late cognitive

dysfunction affects the electroencephalogram in Parkinson's disease. Parkinsonism Relat. Disord. 13, 348–354.
Colclough, G., Brookes, M., Smith, S., Woolrich, M., 2015. A symmetric multivariate leakage correction for MEG connectomes. NeuroImage 117, 439–448.
Colclough, G., Woolrich, M., Tewarie, P., Brookes, M., Quinn, A., Smith, S., 2016. How reliable are MEG resting-state connectivity metrics? NeuroImage 138, 284–293.
Czigler, B., Csikos, D., Hidasi, Z., Anna Gaal, Z., Csibri, E., Kiss, E., Salacz, P., Molnar, M., 2008. Quantitative EEG in early Alzheimer's disease patients - power spectrum and complexity features. Int. J. Psychophysiol. 68, 75–80.
van Dellen, E., de Waal, H., van der Flier, W.M., Lemstra, A.W., Slooter, A.J., Smits, L.L., van Straaten, E.C., Stam, C.J., Scheltens, P., 2015. Loss of EEG network efficiency is related to cognitive impairment in dementia with lewy bodies. Mov. Disord. 30, 1785–1793.
Desikan, R.S., Ségonne, F., Fischl, B., Quinn, B.T., Dickerson, B.C., Blacker, D., Buckner, R.L., Dale, A.M., Maguire, R.P., Hyman, B.T., 2006. An automated labeling system for subdividing the human cerebral cortex on MRI scans into gyral based regions of interest. NeuroImage 31, 968–980.
Dubbelink, K.T.O., Stoffers, D., Deijen, J.B., Twisk, J.W., Stam, C.J., Berendse, H.W., 2013. Cognitive decline in Parkinson's disease is associated with slowing of resting-state brain activity: a longitudinal study. Neurobiol. Aging 34, 408–418.
Dujardin, K., Moonen, A.J., Behal, H., Defebvre, L., Duhamel, A., Duits, A.A., Plomhause, L., Tard, C., Leentjens, A.F., 2015. Cognitive disorders in Parkinson's disease: confirmation of a spectrum of severity. Parkinsonism Relat. Disord. 21, 1299–1305.
Emre, M., Aarsland, D., Brown, R., Burn, D.J., Duyckaerts, C., Mizuno, Y., Broe, G.A., Cummings, J., Dickson, D.W., Gauthier, S., 2007. Clinical diagnostic criteria for dementia associated with Parkinson's disease. Mov. Disord. 22, 1689–1707.
Finger, H., Bönstrup, M., Cheng, B., Messé, A., Hilgetag, C., Thomalla, G., Gerloff, C., König, P., 2016. Modeling of large-scale functional brain networks based on structural connectivity from DTI: comparison with EEG derived phase coupling networks and evaluation of alternative methods along the modeling path. PLoS Comput. Biol. 12, e1005025.
Fischl, B., 2012. FreeSurfer. NeuroImage 62, 774–781.
Fonseca, L.C., Tedrus, G.M., Letro, G.H., Bossoni, A.S., 2009. Dementia, mild cognitive impairment and quantitative EEG in patients with Parkinson's disease. Clin. EEG Neurosci. 40, 168–172.
Fonseca, L.C., Tedrus, G.M., Carvas, P.N., Machado, E.C., 2013. Comparison of quantitative EEG between patients with Alzheimer's disease and those with Parkinson's disease dementia. Clin. Neurophysiol. 124, 1970–1974.
Fornito, A., Bullmore, E.T., 2015. Connectomics: a new paradigm for understanding brain disease. Eur. Neuropsychopharmacol. 25, 733–748.
Fornito, A., Yoon, J., Zalesky, A., Bullmore, E.T., Carter, C.S., 2011. General and specific functional connectivity disturbances in first-episode schizophrenia during cognitive control performance. Biol. Psychiatry 70, 64–72.
Fornito, A., Zalesky, A., Breakspear, M., 2015. The connectomics of brain disorders. Nat. Rev. Neurosci. 16, 159–172.
Franciotti, R., Iacono, D., Della Penna, S., Pizzella, V., Torquati, K., Onofrj, M., Romani, G., 2006. Cortical rhythms reactivity in AD, LBD and normal subjects: a quantitative MEG study. Neurobiol. Aging 27, 1100–1109.
Gibb, W., Lees, A., 1988. The relevance of the Lewy body to the pathogenesis of idiopathic Parkinson's disease. J. Neurol. Neurosurg. Psychiatry 51, 745–752.
Goetz, C.G., Tilley, B.C., Shaftman, S.R., Stebbins, G.T., Fahn, S., Martinez-Martin, P., Poewe, W., Sampaio, C., Stern, M.B., Dodel, R., Dubois, B., Holloway, R., Jankovic, J., Kulisevsky, J., Lang, A.E., Lees, A., Leurgans, S., LeWitt, P.A., Nyenhuis, D., Olanow, C.W., Rascol, O., Schrag, A., Teresi, J.A., van Hilten, J.J., LaPelle, N., Movement Disorder Society, U.R.T.F., 2008. Movement Disorder Society-sponsored revision of the Unified Parkinson's Disease Rating Scale (MDS-UPDRS): scale presentation and clinimetric testing results. Mov. Disord. 23, 2129–2170.
Gramfort, A., Papadopoulo, T., Olivi, E., Clerc, M., 2010. OpenMEEG: opensource software for quasistatic bioelectromagnetics. Biomed. Eng. Online 9, 45.
Gratton, G., Coles, M.G., Donchin, E., 1983. A new method for off-line removal of ocular artifact. Electroencephalogr. Clin. Neurophysiol. 55, 468–484.
Graves, R.E., Bezeau, S.C., Fogarty, J., Blair, R., 2004. Boston naming test short forms: a comparison of previous forms with new item response theory based forms. J. Clin. Exp. Neuropsychol. 26, 891–902.
Guye, M., Bettus, G., Bartolomei, F., Cozzone, P.J., 2010. Graph theoretical analysis of structural and functional connectivity MRI in normal and pathological brain networks. MAGMA 23, 409–421.
de Haan, W., Pijnenburg, Y.A., Strijers, R.L., van der Made, Y., van der Flier, W.M., Scheltens, P., Stam, C.J., 2009. Functional neural network analysis in frontotemporal dementia and Alzheimer's disease using EEG and graph theory. BMC Neurosci. 10, 101.
Halliday, G.M., McCann, H., 2010. The progression of pathology in Parkinson's disease. Ann. N. Y. Acad. Sci. 1184, 188–195.
Hamilton, M., 1960. A rating scale for depression. J. Neurol. Neurosurg. Psychiatry 23, 56–62.
Harrington, D.L., Rubinov, M., Durgerian, S., Mourany, L., Reece, C., Koenig, K., Bullmore, E., Long, J.D., Paulsen, J.S., Rao, S.M., 2015. Network topology and functional connectivity disturbances precede the onset of Huntington's disease. Brain 138, 2332–2346.
Hassan, M., Wendling, F., 2015. Tracking dynamics of functional brain networks using dense EEG. IRBM 36, 324–328.
Hassan, M., Dufor, O., Merlet, I., Berrou, C., Wendling, F., 2014. EEG source connectivity analysis: from dense array recordings to brain networks. PLoS One 9, e105041.
Hassan, M., Benquet, P., Biraben, A., Berrou, C., Dufor, O., Wendling, F., 2015a. Dynamic reorganization of functional brain networks during picture naming. Cortex 73, 276–288.
Hassan, M., Shamas, M., Khalil, M., El Falou, W., Wendling, F., 2015b. EEGNET: an open source tool for analyzing and visualizing M/EEG connectome. PLoS One 10, e0138297.
Hassan, M., Merlet, I., Mheich, A., Kabbara, A., Biraben, A., Nica, A., Wendling, F., 2016. Identification of interictal epileptic networks from dense-EEG. Brain Topogr. 1–17.
He, Y., Chen, Z., Evans, A., 2008. Structural insights into aberrant topological patterns of large-scale cortical networks in Alzheimer's disease. J. Neurosci. 28, 4756–4766.
Hipp, J.F., Hawellek, D.J., Corbetta, M., Siegel, M., Engel, A.K., 2012. Large-scale cortical correlation structure of spontaneous oscillatory activity. Nat. Neurosci. 15, 884–890.
Hoehn, M.M., Yahr, M.D., 2001. Parkinsonism: onset, progression, and mortality. 1967. Neurology 57, S11–S26.
Kamei, S., Morita, A., Serizawa, K., Mizutani, T., Hirayanagi, K., 2010. Quantitative EEG analysis of executive dysfunction in Parkinson disease. J. Clin. Neurophysiol. 27, 193–197.
Klimesch, W., 1999. EEG alpha and theta oscillations reflect cognitive and memory performance: a review and analysis. Brain Res. Rev. 29, 169–195.
Lachaux, J.-P., Rodriguez, E., Martinerie, J., Varela, F.J., 1999. Measuring phase synchrony in brain signals. Hum. Brain Mapp. 8, 194–208.
de Lau, L.M., Breteler, M.M., 2006. Epidemiology of Parkinson's disease. Lancet Neurol. 5, 525–535.
Leentjens, A.F., Dujardin, K., Pontone, G.M., Starkstein, S.E., Weintraub, D., Martinez-Martin, P., 2014. The Parkinson Anxiety Scale (PAS): development and validation of a new anxiety scale. Mov. Disord. 29, 1035–1043.
Li, H., Xue, Z., Ellmore, T.M., Frye, R.E., Wong, S.T., 2014. Network-based analysis reveals stronger local diffusion-based connectivity and different correlations with oral language skills in brains of children with high functioning autism spectrum disorders. Hum. Brain Mapp. 35, 396–413.
Liao, W., Zhang, Z., Pan, Z., Mantini, D., Ding, J., Duan, X., Luo, C., Lu, G., Chen, H., 2010. Altered functional connectivity and small-world in mesial temporal lobe epilepsy. PLoS One 5, e8525.
Lo, C.-Y., Wang, P.-N., Chou, K.-H., Wang, J., He, Y., Lin, C.-P., 2010. Diffusion tensor tractography reveals abnormal topological organization in structural cortical networks in Alzheimer's disease. J. Neurosci. 30, 16876–16885.
Lopes, R., Delmaire, C., Defebvre, L., Moonen, A.J., Duits, A.A., Hofman, P., Leentjens, A.F., Dujardin, K., 2017. Cognitive phenotypes in Parkinson's disease differ in terms of brain-network organization and connectivity. Hum. Brain Mapp. 38, 1604–1621.
Lynall, M.-E., Bassett, D.S., Kerwin, R., McKenna, P.J., Kitzbichler, M., Muller, U., Bullmore, E., 2010. Functional connectivity and brain networks in schizophrenia. J. Neurosci. 30, 9477–9487.
Mallio, C.A., Schmidt, R., Reus, M.A., Vernieri, F., Quintiliani, L., Curcio, G., Beomonte Zobel, B., Quattrocchi, C.C., den Heuvel, M.P., 2015. Epicentral disruption of structural connectivity in Alzheimer's disease. CNS Neurosci. Ther. 21, 837–845.
Morris, J.C., 1993. The Clinical Dementia Rating (CDR): current version and scoring rules. Neurology 43, 2412–2414.
Olde Dubbelink, K.T., Hillebrand, A., Stoffers, D., Deijen, J.B., Twisk, J.W., Stam, C.J., Berendse, H.W., 2014. Disrupted brain network topology in Parkinson's disease: a longitudinal magnetoencephalography study. Brain 137, 197–207.
Oostenveld, R., Praamstra, P., 2001. The five percent electrode system for high-resolution EEG and ERP measurements. Clin. Neurophysiol. 112, 713–719.
de Pasquale, F., Della Penna, S., Snyder, A.Z., Marzetti, L., Pizzella, V., Romani, G.L., Corbetta, M., 2012. A cortical core for dynamic integration of functional networks in the resting human brain. Neuron 74, 753–764.
Penttila, M., Partanen, J.V., Soininen, H., Riekkinen, P.J., 1985. Quantitative analysis of occipital EEG in different stages of Alzheimer's disease. Electroencephalogr. Clin. Neurophysiol. 60, 1–6.
Pievani, M., de Haan, W., Wu, T., Seeley, W.W., Frisoni, G.B., 2011. Functional network disruption in the degenerative dementias. Lancet Neurol. 10, 829–843.
Ponten, S., Bartolomei, F., Stam, C., 2007. Small-world networks and epilepsy: graph theoretical analysis of intracerebrally recorded mesial temporal lobe seizures. Clin. Neurophysiol. 118, 918–927.
Reid, W., Hely, M., Morris, J., Loy, C., Halliday, G., 2011. Dementia in Parkinson's disease: a 20-year neuropsychological study (Sydney Multicentre Study). J. Neurol. Neurosurg. Psychiatry 2010, 232678.
Reitan, R.M., Wolfson, D., 1995. Category Test and Trail Making Test as measures of frontal lobe functions. Clin. Neuropsychol. 9, 50–56.
Roh, J.H., Park, M.H., Ko, D., Park, K.W., Lee, D.H., Han, C., Jo, S.A., Yang, K.S., Jung, K.Y., 2011. Region and frequency specific changes of spectral power in Alzheimer's disease and mild cognitive impairment. Clin. Neurophysiol. 122, 2169–2176.
Rubinov, M., Sporns, O., 2010. Complex network measures of brain connectivity: uses and interpretations. NeuroImage 52, 1059–1069.
Schoffelen, J.M., Gross, J., 2009. Source connectivity analysis with MEG and EEG. Hum. Brain Mapp. 30, 1857–1865.
Skidmore, F., Korenkevych, D., Liu, Y., He, G., Bullmore, E., Pardalos, P.M., 2011. Connectivity brain networks based on wavelet correlation analysis in Parkinson fMRI data. Neurosci. Lett. 499, 47–51.
Skidmore, F., Yang, M., Baxter, L., Von Deneen, K., Collingwood, J., He, G., White, K., Korenkevych, D., Savenkov, A., Heilman, K., 2013. Reliability analysis of the resting state can sensitively and specifically identify the presence of Parkinson disease. NeuroImage 75, 249–261.
Smith, A., 1982. Symbol Digit Modalities Test (SDMT) Manual (Revised). Western Psychological Services, Los Angeles.
Sockeel, P., Dujardin, K., Devos, D., Deneve, C., Destee, A., Defebvre, L., 2006. The Lille apathy rating scale (LARS), a new instrument for detecting and quantifying apathy: validation in Parkinson's disease. J. Neurol. Neurosurg. Psychiatry 77, 579–584.
Song, S.K., Lee, J.E., Park, H.J., Sohn, Y.H., Lee, J.D., Lee, P.H., 2011. The pattern of cortical atrophy in patients with Parkinson's disease according to cognitive status. Mov. Disord. 26, 289–296.
Stam, C., Jones, B., Nolte, G., Breakspear, M., Scheltens, P., 2007. Small-world networks and functional connectivity in Alzheimer's disease. Cereb. Cortex 17, 92–99.
Steriade, M., Gloor, P., Llinas, R.R., Da Silva, F.L., Mesulam, M.-M., 1990. Basic mechanisms of cerebral rhythmic activities. Electroencephalogr. Clin. Neurophysiol. 76, 481–508.

Stoffers, D., Bosboom, J.L., Deijen, J.B., Wolters, E.C., Berendse, H.W., Stam, C.J., 2007. Slowing of oscillatory brain activity is a stable characteristic of Parkinson's disease without dementia. Brain 130, 1847–1860.

Stoffers, D., Bosboom, J., Deijen, J., Wolters, E.C., Stam, C.J., Berendse, H., 2008. Increased cortico-cortical functional connectivity in early-stage Parkinson's disease: an MEG study. NeuroImage 41, 212–222.

Tadel, F., Baillet, S., Mosher, J.C., Pantazis, D., Leahy, R.M., 2011. Brainstorm: a user-friendly application for MEG/EEG analysis. Comput. Intell. Neurosci. 2011, 8.

Tomlinson, C.L., Stowe, R., Patel, S., Rick, C., Gray, R., Clarke, C.E., 2010. Systematic review of levodopa dose equivalency reporting in Parkinson's disease. Mov. Disord. 25, 2649–2653.

Tröster, A.I., 2011. A précis of recent advances in the neuropsychology of mild cognitive impairment(s) in Parkinson's disease and a propo sal of preliminary research criteria. J. Int. Neuropsychol. Soc. 17, 393–406.

Utianski, R.L., Caviness, J.N., van Straaten, E.C.W., Beach, T.G., Dugger, B.N., Shill, H.A., Driver-Dunckley, E.D., Sabbagh, M.N., Mehta, S., Adler, C.H., 2016. Graph theory network function in Parkinson's disease assessed with electroencephalography. Clin. Neurophysiol. 127, 2228–2236.

Van de Steen, F., Faes, L., Karahan, E., Songsiri, J., Sosa, P.A.V., Marinazzo, D., 2016. Critical comments on EEG sensor space dynamical connectivity analysis. arXiv preprint arXiv:1607.03687.

Wechsler, D., 1981. WAIS-R:[Wechsler Adult Intelligence Scale-Revised]. Psychological Corporation.

Zalesky, A., Fornito, A., Bullmore, E.T., 2010a. Network-based statistic: identifying differences in brain networks. NeuroImage 53, 1197–1207.

Zalesky, A., Fornito, A., Harding, I.H., Cocchi, L., Yücel, M., Pantelis, C., Bullmore, E.T., 2010b. Whole-brain anatomical networks: does the choice of nodes matter? NeuroImage 50, 970–983.

Zhang, Y., Schuff, N., Du, A.T., Rosen, H.J., Kramer, J.H., Gorno-Tempini, M.L., Miller, B.L., Weiner, M.W., 2009. White matter damage in frontotemporal dementia and Alzheimer's disease measured by diffusion MRI. Brain 132, 2579–2592.

Zhang, Z., Liao, W., Chen, H., Mantini, D., Ding, J.-R., Xu, Q., Wang, Z., Yuan, C., Chen, G., Jiao, Q., 2011. Altered functional–structural coupling of large-scale brain networks in idiopathic generalized epilepsy. Brain 134, 2912–2928.